# UWB and Wideband Channel Models for Working Machine Environment

Attaphongse Taparugssanagorn, Matti Hämäläinen, and Jari Iinatti

Centre for Wireless Communications, University of Oulu, Finland

***Abstract*—In this paper, we present statistical models for wideband and ultra-wideband (UWB) radio channels for working machine cabin environment. Based on a set of measurements, it was found that such a small and confined space causes mostly diffuse multipath scattering rather than specular paths. The amplitude of the channel impulse responses in the wideband case is mostly Rayleigh distributed small-scale fading signal, with only few paths exhibiting Ricean distributions, whereas the ones in the UWB case tend to be log-normally distributed. For the path amplitude, we suggest an exponential decay profile, which has a constant slope in dB scale, with the corresponding parameters for the UWB case. For the wideband case, a two-fold exponential decay profile provides excellent fits to the measured data. It was also noted that the root-mean-square (RMS) delay spread is independent of line-of-sight (LOS)/obstructed line-of-sight (OLOS) situations of the channel. The multipath components contributing significant energy play a major role in such a small environment if compared to the direct path. In addition, the radio channel gains are attenuated with the presence of a driver inside the cabin.**

## I. Introduction

Wireless intra-vehicle communications has been proposed as a new type of communications mechanism that can provide onboard passengers with bidirectional high-speed data exchange services for both communications and entertainment [1]. For the purpose of safety, comfort and convenience, new models of automotives to collect such information as temperature, speed, pressure, and so on have also been deployed. This idea is not limited to regular car applications but is also applied in working machines. The information and communication system used in a working machine makes it easier for driver to control operations like guiding the trunk cutting process according to orders in a harvester case. This can guarantee quick processing during logging, and high productivity. This information system is expected to be wirelessly controlled by the driver. Using wireless communication links instead of wired link can save a big amount of installing costs. In addition, measuring vibrations acting on the human body, so-called "human vibration", is the prevention of health risks and the evaluation of comfort, for example in vehicles [2]. Wireless vibration sensing application embedded to wireless body area networks (WBANs) can also be included in the future system.

The design of such a wireless system requires a good understanding of the corresponding radio wave propagation channel. The characteristics of an indoor radio propagation is extremely site-specific. Many existing radio channel measurement campaigns and the corresponding channel models have been restricted to typical residential and office environments, which are highly limited by the attenuation of walls [3, 4]. Only few radio channel measurements were done inside a vehicle [5, 6]. To our knowledge, there is no work done in working machine environments, which have completely different radio channel characteristics due to their small and confined space and dissimilar materials.

This paper discusses on experimental radio channel measurements that are carried out in a working machine environment within two different frequency bands, i.e., the industrial, scientific and medical (ISM) radio frequency band (2.4-2.4835 GHz) and the ultra wideband (UWB) frequency band (3.1-10 GHz). The channel models based on the measurement results are then developed and verified in Matlab. The channel models are targeted for data communication system design for inside cabin applications. Even inside a cabin of a working machine, there are interests to replace wired links with wireless to reduce manufacturing costs and also the weight of the machine.

## II. Measurement Campaigns

### A. Measurement Setup

The measurements were carried out in a frequency domain using Agilent 8720ES S-parameter vector network analyzer (VNA) [7]. The network analyzer is operated in a transfer function measurement mode ($S_{21}$), where port 1 and port 2 are the transmitting and the receiving ports, respectively. Thus, the measurements' result is a frequency response of the channel.

The measurements were carried out in the ISM frequency band at 2.4-2.4835 GHz, which is used, i.e., by the standards IEEE 802.11 and 802.15.4 dedicated for wireless local area network (WLAN) communication. The measurements in an ultra wideband frequency band between 3.1-10 GHz were also carried out. Therefore, the measured bandwidths $B$ were 83.5 MHz and 6.9 GHz, respectively. Consequently, the corresponding delay resolutions are 11.97 ns and 0.14 ns.

The antennas used in the measurements in WLAN band were HGA7S 7 dBi high gain antennas [8]. SkyCross SMT-3TO10M-A antennas [9] were used for the measurements in UWB band. Both types of the antennas are linearly polarized. The SkyCross SMT-3TO10M-A antennas are azimuthally omni-directional, whereas the HGA7S 7 dBi high gain antennas are designed for 360 degrees of coverage [8]. The transmit power used in this study was 5 dBm (equivalent to 3.16 mW) measured at the VNA output port.

978-1-4244-8329-7/11/$26.00 ©2011 IEEE

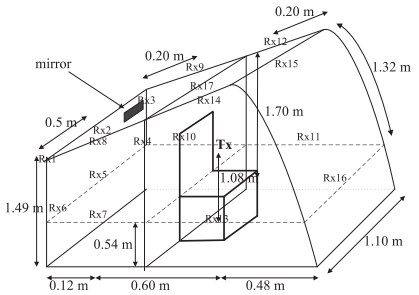


Fig. 1. Arrangement of the antennas' positions for measurements inside a working machine cabin

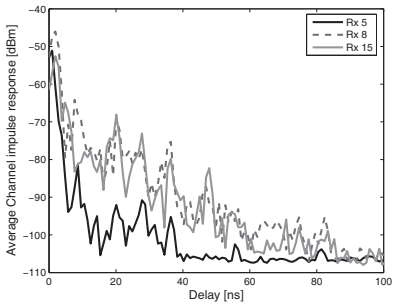


Fig. 2. Average channel impulse responses for the ISM band in Scenario 1: without driver, engine off. Rx positions Rx5, Rx8, and Rx15.

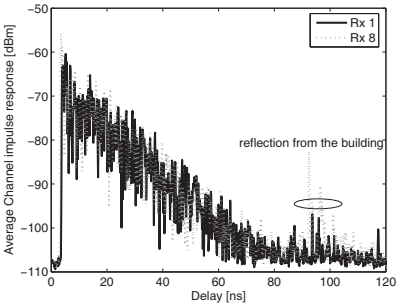


Fig. 3. Average channel impulse responses for UWB band in Scenario 1: without driver, engine is off. Rx positions Rx1 and Rx8.

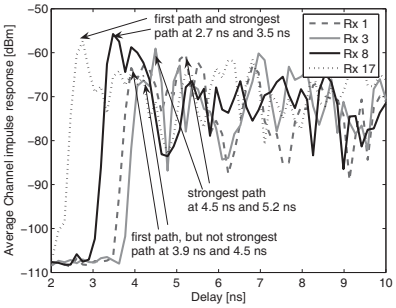


Fig. 4. First path arriving Rx, UWB band in scenario 1, Rx positions Rx1 (OLOS), Rx3 (OLOS), Rx8 (LOS), and Rx17 (LOS).

### *B. Channel Measurement Description*

The measurements were conducted inside a cabin of a working machine with the dimensions as illustrated in Fig. 1. The transmit (Tx) antenna and the receive (Rx) antenna are, in general, set to face each other and the line-of-sight (LOS) path always exists except when the links are blocked by the seat. The position of the Tx antenna is fixed at the seat on 1.08 m above the cabin floor. The positions of the Rx antenna were moved to 17 different spots, namely from the position Rx1 till the position Rx17 at Fig. 1. At each position, 100 consecutive measurements of the channel's frequency response were taken. Each sweep consists of 1601 frequency points, which set the sweep time to 800 ms. In order to study radio channels inside a cabin in a working machine for real situations, three following scenarios were investigated: (1) without a driver, the engine is off, (2) with a driver sitting, the engine is off, and (3) with a driver sitting, the engine is on.

## III. Channel Measurement Results and Data Analysis

Measured ($S_{21}$)-parameters are converted to channel impulse responses $h(\tau)$ using an inverse fast Fourier transform (IFFT). A Hamming window is used to reduce sidelobes. One hundred individual realizations of the channel impulse response were averaged for each position. The average measured channel impulse responses for the ISM band in scenario 1 for the Rx positions Rx5, Rx8 and Rx15 are shown in Fig. 2. The propagation delay, which is the time from 0 ns to the first path, is shown in the channel impulse response plots. The channel impulse responses have two constant slopes in dB scale, which correspond to a typical exponential decay profile in a linear scale. This shows that there are many reflections rather than a significant specular propagation path inside a cabin. This is excellently suited to characterize diffuse scattering [10]. As expected from the antenna positions in Fig. 1, the average channel impulse response for the case when the Rx antenna is at Rx5 is lower than the others since the LOS signal is obstructed by the seat. The results of the measurements can be classified into two sub-scenarios, namely, an LOS for the Rx positions 8, 9, 11-17 and an obstructed line-of-sight (OLOS) for the Rx positions 1-6, 7, 10.

Fig. 3 compares the average channel impulse responses for the UWB band in Scenario 1. The Rx positions are Rx1 and Rx8. The UWB measurements allows to distinguish the presence of numerous paths arriving at the receiver due to its fine delay resolution. The UWB channel impulse responses have a constant slope in dB. The reflections from the building nearby the working machine appear small peaks at about 92 ns, which is 27.6 m or exactly twice the distance between the working machine and the building (13.8 m). Nevertheless, these peaks are not in our consideration since they are outside the range of the cabin. However, these peaks confirm the scaling of the presented impulse responses.

The other advantage of the UWB measurements is the high temporal resolution, which makes it possible to see the first

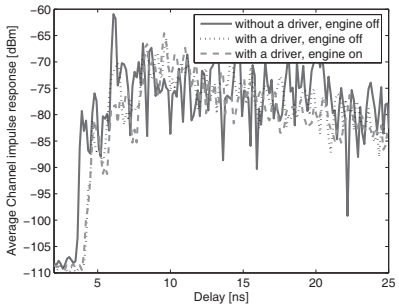


Fig. 5. Average measured channel impulse responses for UWB band, Rx5 (OLOS), three different scenarios.

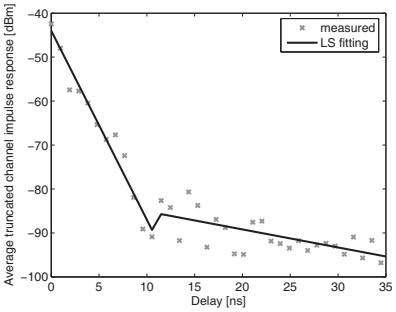


Fig. 6. Average channel impulse responses for ISM band, Rx17 (LOS) and the least square (LS) linear fitting curve in dB scale.

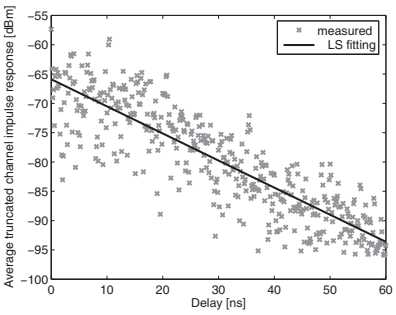


Fig. 7. Average channel impulse responses for UWB band, Rx17 (LOS) and the least square (LS) linear fitting curve in dB scale.

path more precisely. Fig. 4 presents the examples of the first paths arriving at the receiver in Scenario 1 for four different Rx positions, Rx1, Rx3, Rx8, and Rx17. The first path arrival time can approximately translate into the distance between Tx and Rx antennas. Therefore, the distances between Tx and Rx1, Rx3, Rx8 and Rx17 are 1.17 m, 1.35 m, 1.05 m, and 0.81 m, respectively (3.9 ns, 4.5 ns, 3.5 ns, and 2.7 ns, respectively). The Rx1 and Rx3 are OLOS cases, thus the first path is not the strongest path. Depending on the position, the constructive multipaths can create a stronger path to the receiver. The Rx8 and Rx17 are LOS cases, therefore the first path is also the strongest path. Fig. 5 is an example of the comparison of the results in three defined different scenarios for UWB band. When the driver is inside the cabin, the radio waves in all multipaths from the Tx close to the body of the driver (≈3 cm) are attenuated. In addition, the first path arrival time is longer than the one in the case of no driver inside the cabin. No significant difference is found between the engine is on and off cases, i.e., vibration has no impact on the radio propagation channels, as it should not have.

### *A. Exponential Decaying Factor ($a_l$)*

The path amplitude $a_l$ is approximately modeled by an exponential decay profile with a Ricean factor $\gamma_0$ and an exponential decaying factor $\Gamma$ for UWB case as

$$E\{10\log_{10}|a_l|\} = \begin{cases} 0, & l=0 \\ \gamma_0 + 10\log_{10}\left(\exp\left(\frac{-t_l}{\Gamma}\right)\right), & 1 \le l \le L-1 \end{cases}, \quad (1)$$

where $E\{\cdot\}$ is the expectation value and $L$ is the number of paths. For ISM case, the channel impulse responses have two constant slopes in dB scale, and thus the $a_l$ is approximately modeled by two-fold exponential decay profile with two Ricean factors $\gamma_{01}$ and $\gamma_{02}$ as well as two exponential decaying factors $\Gamma_1$ and $\Gamma_2$ as

$$E\{10\log_{10}|a_l|\} = \begin{cases} 0, & l=0 \\ \gamma_{01} + 10\log_{10}\left(\exp\left(\frac{-t_l}{\Gamma_1}\right)\right), & 1 \le l \le l_1 \\ \gamma_{02} + 10\log_{10}\left(\exp\left(\frac{-t_l}{\Gamma_2}\right)\right), & l_1+1 \le l \le L-1 \end{cases}, \quad (2)$$

where $l_1$ is the last path of the first cluster.

Fig. 6 shows the average channel impulse response for the ISM band (Rx17, LOS) in the first scenario (without a driver, the engine is off) and the two-fold least square (LS) linear fitting curve in dB scale. The corresponding factors $\gamma_{01}$ and $\gamma_{02}$ are -44 dB and -81 dB, respectively, and the exponential decaying factors $\Gamma_1$ and $\Gamma_2$ are 2.33 and 24.39, respectively. Fig. 7 shows the average channel impulse response for the UWB band (Rx17, LOS) and the least square (LS) linear fitting in dB scale. The corresponding factor $\gamma_0$ and the exponential decaying factor $\Gamma$ are -66 dB and 21.74.The amplitude variations $\chi$ over the mean values of the path amplitudes are well fitted by the log-normal distribution with zero-mean and standard deviation $\sigma_\chi$ of 6.69 dB and 4.50 dB, respectively. The number of paths above the noise threshold, $L$, for Rx14 (LOS) and Rx5 (OLOS) in the UWB band are excellently fitted by Poisson distribution with a mean $\mu_L$. The number of paths is smaller in OLOS and decreased with the presence of the driver. In the case of the ISM band, the number of paths $L$ are fitted by Gaussian distribution with a mean $\mu_L$ and a standard deviation $\sigma_L$. In addition, the number of paths is changed quite dramatically when the engine is changed from off to on (thus, including in cabin vibration) in the case of LOS. However, the difference is not much in OLOS case. The number of paths presented in the paper are for channel modeling purpose. Nonetheless, modeling shows much more paths than the typical number of paths obtained

during a system design, i.e., the number of paths within 10 dB of the strongest path or the number of paths containing 85 percent of the energy, which gives approximately 35-50 paths.

### B. Small-Scale Channel Characterization

*1) Delay Dispersion:* In order to compare different multipath channels and to develop general design guidelines, parameters which grossly quantify the multipath channel are used. The mean excess delay $\tau_{\mathrm{m}}$ and root-mean-square (RMS) delay spread $\tau_{\mathrm{RMS}}$ are commonly used to imply the time delay dispersive properties of a wideband multipath channel parameters that can be determined from a power delay profile [11].

The measured RMS delay spreads for LOS and OLOS situations for the UWB band measurements are in the range of 1.7-5.8 ns, which are very small if compared to typical indoor RMS delay spread varying between 14 to 18 ns [11]. We can see that the RMS delay spread is independent of the LOS/OLOS situations of the channel. Neither of the distance, this is because the cabin space is relative small. The multipath components contributing significant energy play a major role in such a small environment if compared to the direct path. This is very important on the selection of the antenna position and also at the receiver design. The RMS delay spread for the case of the cabin with a driver decreases by approximately 1.2 ns, since the presence of people in the cabin attenuates some propagation paths. In addition, the standard deviations $\sigma$ of the RMS delay spreads, when the engine is on (cabin vibration) are larger than the ones when the engine is off.

*2) Amplitude Distribution:* In the ISM band (83.5 MHz bandwidth), the power received for each delay tap is the vectorial sum of many multipath components arriving in the corresponding delay bin. The central limit theorem is therefore valid and the amplitudes of the delay bins exhibit a Rayleigh (in non LOS or OLOS cases) or a Ricean (in LOS case) distribution. On the contrary, only few multipath components (MPCs) fall into each resolvable delay in the UWB band (6.9 GHz bandwidth). Therefore, the central limit theorem is not applicable and the amplitudes of the delay bins consequently do not exhibit a Rayleigh or Rice distributions. As an example, the CDFs of amplitudes of some delay bins in the ISM band for the LOS case at Rx12 are shown in Fig. 8. The measured amplitudes of each delay bin are excellently fitted by a Ricean distribution with the probability density function (PDF) given by

$$p(r) = \frac{r}{\sigma^2} \exp\left(-\left(r^2 + A^2\right)/2\sigma^2\right) I_0\left(\frac{Ar}{\sigma^2}\right), \qquad (3)$$

where $A$ denotes the peak amplitude of the dominant signal, $I_0$ is the modified Bessel function of the first kind and zero-order, and $\sigma^2$ is the time-average power of the received signal before envelope detection. The corresponding $K$-factor is the ratio between the deterministic signal power and the variance of the multipath, and is defined by

$$K\,[dB] = 10 \log_{10}\left(\frac{A^2}{2\sigma^2}\right). \qquad (4)$$

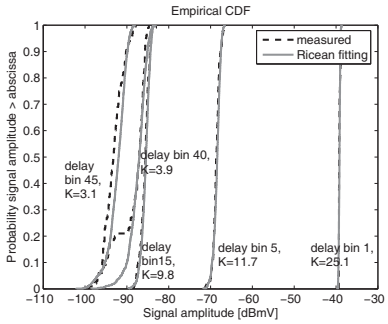


Fig. 8. CDFs of the amplitudes of five delay bins, 1, 5, 15, 40 and 45 with corresponding $K$-factors for Rx12 (LOS).

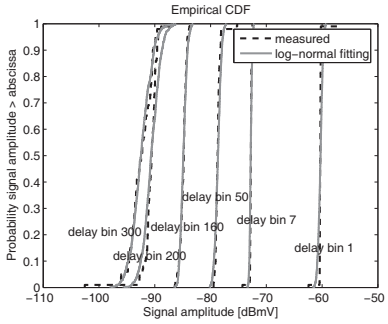


Fig. 9. CDFs of the amplitudes of four delay bins, 1, 5, 15, and 40 with log-normal fitting for Rx1 (OLOS), without driver, engine off.

When $A \to 0$, $K \to -\infty$ dB, and as the dominant path decreases in amplitude, the Ricean distribution degenerates to a Rayleigh distribution.

With the presence of a driver in the ISM band case, the first delay bins tend to be Ricean distributed due to their high $K$-factors, whereas the other delay bins can be assumed to be Rayleigh distributed due to their very small $K$-factors.

Fig. 9 illustrates the analysis for LOS case in the UWB band. As explained above, only few MPCs fall into each resolvable delay and the central limit theorem is therefore not applicable. The measured amplitudes of all delay bins (for example, the delay bins 1, 7, 50, 160, 200, and 300) consequently do not exhibit a Rayleigh or a Ricean distribution, but are rather log-normally distributed with a certain mean $\mu$ (-60.3, -72.8, -78.7, -84.9, and -90.7 dBmV) and standard deviations $\sigma$ (0.40, 0.56, 0.21, 0.57, 1.48, and 1.87 dB), respectively.

## IV. Channel Modeling and Evaluation

Based on the measurement results, channel models for cabin environment are developed in Matlab. As shown in Figs. 8-9 in subsection III-B2, the amplitudes of the first five delay bins in the ISM band case for the LOS case tends to be Ricean distributed. The remaining delay bins can be assumed to be Rayleigh distributed due to their small $K$-factors. For the OLOS case, only the first delay bin tends to be Ricean distributed, whereas the rest can be assumed to be Rayleigh distributed. In the UWB case, the amplitudes of all delay bins

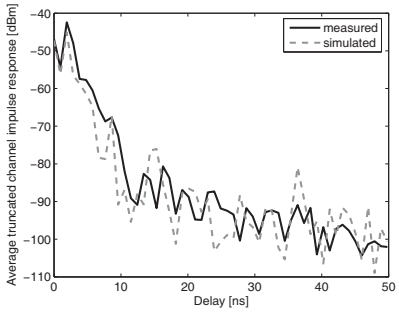


Fig. 10. Average measured and simulated channel impulse responses for Rx17 (LOS), ISM band.

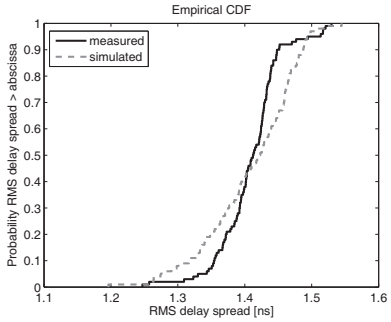


Fig. 11. CDF of the RMS delay spreads of the measured and simulated channels for Rx17 (LOS), ISM band.

are log-normally distributed. Subsequently, the path amplitude is obtained by using the analyzed exponential decay profile with the corresponding Ricean factor $\gamma_0$ and exponential decaying factor $\Gamma$ described in subsection III-A.

As an example, the channels for the case of Rx17 (LOS) in the ISM band and the case of Rx17 (LOS) in the UWB band (Figs. 6 and 7) are simulated. For the former case, it is done by using (1) and the simulation parameters presented in Table I. For the latter case, (2) is used with the simulation parameters in Table I. The average channel impulse response and the RMS delay spread $\tau_{\mathrm{RMS}}$ are used for validating the simulated model as depicted in Figs. 10-11. As we can see, the simulated channels have a good agreement with the measured channels.

TABLE I
MEASUREMENT SYSTEM PARAMETERS FOR THE CASE OF RX 17 (LOS).

| **Parameters** | **ISM Band** | **UWB Band** |
|---|---|---|
| $\mu_L$ [paths] | 53 | 441 |
| $\gamma_{01}$ [dB] | -44 | - |
| $\gamma_{02}$ [dB] | -81 | - |
| $\gamma_0$ [dB] | - | -66 |
| $\Gamma_1$ | 2.33 | - |
| $\Gamma_2$ | 24.39 | - |
| $\Gamma$ | - | 21.74 |
| Amplitude distribution | Ricean with $K$-factor = 21.35, 16.70, 16.28, 14.40, 13.89 dB for the delay bin 1-5, Rayleigh for the remaining delay bins | log-normal for all delay bins |
| $\sigma_\chi$ [dB] | 2.97 and 3.04 | 4.50 |

## V. CONCLUSIONS

The channel models based on the measurements in a working machine cabin environment were developed for two different frequency bands; ISM and UWB bands. The channel characteristics were different from traditional indoor environments, namely, there are many reflections rather than a significant specular path. With the presence of a driver inside the cabin, the channel gains are attenuated. In both frequency ranges, the exponential decay profile was modeled for each path with the corresponding parameters. For the ISM band, the amplitudes of the delay bins exhibit a Rayleigh (in OLOS case) or Ricean (in LOS case) distributions. On the contrary, only few multipath components fall into each resolvable delay bin in the UWB band. Therefore, the central limit theorem is not applicable and the amplitudes of the delay bins consequently do not exhibit a Rayleigh or Ricean distribution, but rather log-normal distribution. The RMS delay spread was independent of the LOS/OLOS situations of the channel in both cases. Neither of the distance, this is because the cabin space is very small. The multipath components contributing significant energy play a major role in such a small environment if compared to the direct path. This is very important on the selection of the antenna position and the receiver design.

## ACKNOWLEDGMENT

The authors would like to thank Mr. Ari Isola for his contribution during the measurements. This work was funded by the Finnish Funding Agency for Technology and Innovation through the European Regional Development Fund.

## REFERENCES

[1] G. Leen and D. Hefferna, "Vehicles without wires," *Automotive Electronics, Computing and Control Engineering Journal*, pp. 205-211, Oct 2001.

[2] AN21E Application Note Human Vibration Measurement EC Directive 2002/44/EC.

[3] D. Cassioli, M. Z. Win, and A. F. Molisch, "The ultra-wide bandwidth indoor channel: From statistical models to simulations," *IEEE J. Selected Areas Communications*, vol. 20, pp. 1247-1257, Aug 2002.

[4] S. Ghassemzadeh, R. Jana, C. Rice, W. Turin, and V. Tarokh, "Measurement and modelling of an ultra-wide bandwidth indoor channel," *IEEE Trans. Communications*, vol. 52, Issue. 10, pp. 1786-1796, Oct. 2004.

[5] W. Niu, J. Li, and T. Talty, "Intra-Vehicle UWB Channel Measurements and Statistical Analysis," in *Proc. IEEE Global Telecommunications Conference*, pp. 1-5, Nov. 2008.

[6] W. Xiang, "A Vehicular Ultra-Wideband Channel Model for Future Wireless Intra-Vehicle Communications (IVC) Systems," in *Proc. IEEE Vehicular Technology Conference Fall*, pp. 2159-2163, Oct. 2007.

[7] http://www.alliancetesteq.com/.

[8] http://tinyurl.com/cyszob.

[9] http://skycross.com/Products/PDFs/SMT-3TO10M-A.pdf.

[10] A. Richter. *Estimation of radio channel parameters: Models and Algorithms*, Ph.D. dissertation, Technische Universitt Ilmenau, Ilmenau, 2005.

[11] A. Muqaibel, A. Safaai-Jazi, A. Attiya, B. Woerner, and S. Riad, "Path-loss and time dispersion parameters for indoor UWB propagation," *IEEE Trans. on Wireless Communications*, vol. 5, no. 3, pp. 550-559, March 2006.